Interaction Types in $C_6H_5(CH_2)_nOH$-CO_2 (n = 0-4) Determined by the Length of Side Alkyl Chain

Hao Wang,[†] Junhua Chen,[†] Yang Zheng,[†] Daniel A. Obenchain,[‡] Xuefang Xu,[†] Qian Gou,[†*] Jens-Uwe Grabow,[§] Walther Caminati[ǁ]

[†] Department of Chemistry, School of Chemistry and Chemical Engineering, Chongqing University, No.55 Daxuecheng South Rd., Shapingba, Chongqing, 401331, China.

[‡] Institut für Physikalische Chemie, Universität Göttingen, Tammannstr. 6, 37077 Göttingen, Germany.

[§] Institut für Physikalische Chemie & Elektrochemie, Leibniz Universität Hannover, Callinstraβe 3A, 30167 Hannover, Germany.

[ǁ] Dipartimento di Chimica "G. Ciamician", Università di Bologna, Via Selmi 2, I-40126 Bologna, Italy.

Corresponding Authors

* Qian Gou: qian.gou@cqu.edu.cn;

Table of Contents

1. Methods

1.1 Experimental measurement

Molecular clusters were generated in a supersonic expansion, under optimized conditions. Details of the Fourier transform microwave (FTMW)[1] spectrometer (COBRA-type),[2] which covers the range 2-20 GHz, have been described previously.[3] A gas mixture of about 1 % of CO_2 (commercial sample used without further purification) in helium at a stagnation pressure of about 0.2 MPa was passed over $C_6H_5(CH_2)_{0\text{-}2}OH$ (phenol/333K, phenylmethanol/353K, and 2-phenylethanol/363K) and expanded through a solenoid valve (General Valve, Series 9, nozzle diameter 0.5 mm) into the Fabry-Pérot cavity (10^{-5} pa), respectively. The spectral line positions were determined after Fourier transformation of the time-domain signal with 8k data points, recorded with 100 ns sample intervals. Each rotational transition appears as a doublet because of the Doppler Effect. The line position is calculated as the arithmetic mean of the frequencies of the Doppler components. The estimated accuracy of the frequency measurements is better than 1 kHz. Line separated by more than 5 kHz are resolvable.

1.2 Theoretical calculations

Structure Optimization. The full geometry optimizations of $C_6H_5(CH_2)_{0\text{-}4}OH\text{-}CO_2$ have been done with DFT at the B3LYP-D3(BJ)/aug-cc-pVTZ level of theory using the Gaussian16 program package.[4] The harmonic frequency calculations were performed at the same level to confirm the real minima and obtain their zero-point vibrational energies. The basis set superposition error (BSSE) were also considered for the binding energies of the complexes.[5] The experimental transition frequencies were fitted to the spectroscopic constants with Pickett's SPFIT program.[6] All observed transition lines were fitted with the Watson's semi-rigid Hamiltonian employing the *S* reduction in I^r representation.[7]

Theoretical molecular structures.

1) Phenol-CO_2:

Isomer I prefers an in-plane configuration with a C···O tetrel bond (TB) and a C-H···O weak hydrogen bond (HB) over the ones that CO_2 locates above the aromatic ring (C···π TBs) as in isomers II and III, differed in the orientation of CO_2.

2) PM/2PE-CO_2:

In case of PM/2PE-CO_2 complexes, the non-covalent interactions and relative energies order of the three isomers are almost the same. The global minima (isomers I) are linked by a C···π and an O-H···O interaction. If C···O TB is formed, the resulting isomers II lie in higher energy with respect to the global minima. If CO_2 is positioned on the opposite side of the hydroxyl group in PM and 2PE, the resulting isomers III are even higher in energies.

3) STRFIT:

The fitting procedure of r_0 structure was performed using the STRFIT program.[8]

NCI calculations. To better visualize the non-covalent interactions in $C_6H_5(CH_2)_{0\text{-}2}OH\text{-}CO_2$, Johnson's NCI analysis which is based on the electron density and its gradients[9] has been applied through Multiwfn.[10] The isosurface plots were visualized by VMD.[11] The global minima of all complexes optimized at the B3LYP-D3(BJ)/aug-cc-pVTZ level of theory were used for the analyses.

PIO analysis calculations. Results of PIO analysis on the phenol-CO_2 complex with phenol and CO_2 as two fragments based on B3LYP-D3(BJ)/aug-cc-pVTZ geometries.[12] The orbital energies and populations (occupation numbers) are given as E and P, respectively. The PIO-based bond indices (abbreviated as PBI) and its contribution (as %) to the total interactions between two fragments (the contributions of all PIOs sum up to 100%) were obtained for comparison. The same method was also applied to the $C_6H_5(CH_2)_{1\text{-}4}OH\text{-}CO_2$ complexes.

SAPT analysis calculations. In order to better understand these sets of interesting NCIs, the energy of the intermolecular interaction has been interpreted in physical meaningful way such as electrostatics, induction, dispersion and exchange-repulsion by using the Symmetry-Adapted Perturbation theory (SAPT).[13] The SAPT analysis has been carried out using PSI4 package at SAPT2+3/aug-cc-pVDZ-RI level.[14]

AIM analysis calculations. In the topological analysis, the bond critical points (BCPs) give detailed information on the nature and relative strength of the hydrogen bonding interactions, obtained in term of electron density (ρ). Intermolecular HBs can be calculated by formulas: $E[\text{kcal mol}^{-1}] = -223.08 \times \rho_{BCP} + 0.7423$.[15]

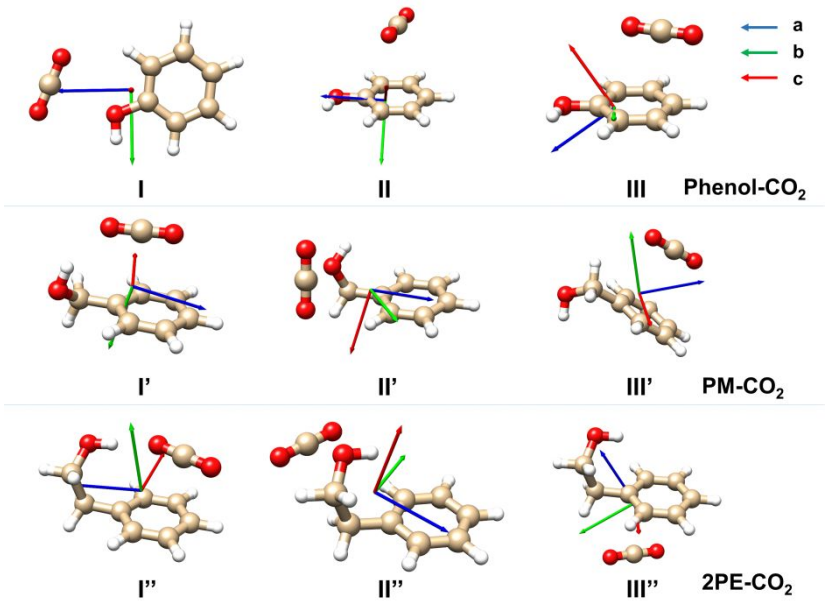

Figure S1 Plausible isomers of $C_6H_5(CH_2)_{0\text{-}2}OH\text{-}CO_2$ calculated at B3LYP-D3(BJ)/aug-cc-pVTZ level of theory with the principal inertial axes.

Table S1a. B3LYP-D3(BJ)/aug-cc-pVTZ spectroscopic parameters of all $C_6H_5(CH_2)_{0\text{-}2}OH\text{-}CO_2$ complexes.

Parameters[a]	C_6H_5OH (phenol)			$C_6H_5CH_2OH$ (PM)			$C_6H_5(CH_2)_2OH$ (2PE)		
	I	II	III	I'	II'	III'	I''	II''	III''
A/MHz	3485	1728	1990	1196	1994	1230	1166	1736	1191
B/MHz	603	1011	922	1055	582	942	750	501	673
C/MHz	514	883	817	720	513	664	567	425	518
μ_a/D	0.9	0.7	0.1	1.2	2.0	0.7	-0.8	1.8	-1.4
μ_b/D	-1.2	-0.2	-0.1	-1.0	-0.2	-1.2	-1.0	-0.5	-0.3
μ_c/D	0	-1.2	1.2	0.8	-0.3	0.9	-0.9	-0.5	0.8
$\Delta E_{0,BSSE}$[b]/kJ mol^{-1}	0	0.5	1.4	0	1.1	3.9	0	1.2	3.9
$D_{e,BSSE}$/kJ mol^{-1}	12.7	11.9	11.0	17.6	16.3	12.6	17.2	16.4	12.7
P_{aa}[c]/uÅ^2	830.2	389.9	456.4	382.7	800.0	443.4	565.9	953.4	651.1
P_{bb}/uÅ^2	145.1	182.5	162.2	319.2	185.1	317.7	325.4	235.8	324.5
P_{cc}/uÅ^2	0.1	110.0	91.8	96.4	68.3	93.1	108.0	55.4	99.8

[a] *A*, *B*, and *C* are rotational constants. μ_a, μ_b, and μ_c are electric dipole moments. $D_{e,BSSE}$ is dissociation energies with BSSE correction. [b] Zero-point relative energy with BSSE corrections, the absolute energies for the global minima are -496.164241 (phenol-CO_2), -535.462950 (PM-CO_2) and -574.770604 (2PE-CO_2) E_h, respectively. [c] Planar moments of inertia $P_{gg} = \sum_i m_i g_i^2$ (g = a, b and c) supply information on the mass distributions along principal axes.

Table S1b. B3LYP-D3(BJ)/aug-cc-pVTZ spectroscopic parameters of all $C_6H_5(CH_2)_3OH$-CO_2 complexes within 5.0 kJ mol^{-1}.

Parameters[a]	$C_6H_5(CH_2)_3OH$ (3PP)−CO_2			
	I (GG'g)[b]	II (GGt)	III (GG'g)	IV (TGt)
Plausible isomers	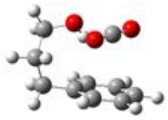		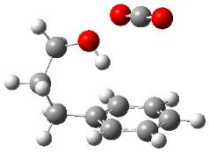	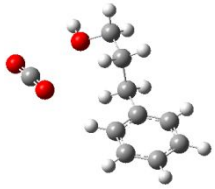
A/MHz	859	1621	854	1364
B/MHz	771	346	747	375
C/MHz	540	329	497	305
μ_a/D	-1.0	0.6	-1.9	0.7
μ_b/D	1.7	−0.3	-0.2	−1.9
μ_c/D	0.7	1.5	1.1	0.3
$\Delta E_{0,BSSE}$[c]/kJ mol^{-1}	0	3.3	3.8	4.0

[a] *A*, *B*, and *C* are rotational constants. μ_a, μ_b, and μ_c are electric dipole moments. [b] Nomenclature of 2PE conformers follows that of ref 16. [c] Zero-point relative energy with BSSE corrections, the absolute energies for the global minima are -614.075122 E_h.

Table S1c. B3LYP-D3(BJ)/aug-cc-pVTZ spectroscopic parameters of all $C_6H_5(CH_2)_4OH$-CO_2 complexes within 5.0 kJ mol^{-1}.

Parameters[a]	$C_6H_5(CH_2)_4OH$ (4PB)−CO_2				
	I	II	III	IV	V
Plausible isomers		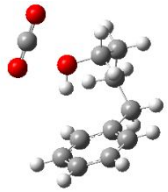	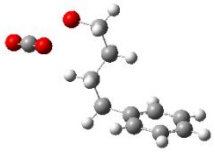	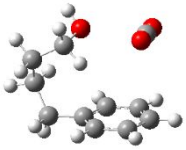	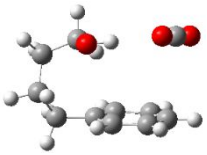
A/MHz	821	996	1377	743	829
B/MHz	603	445	265	638	551
C/MHz	438	380	251	430	415
μ_a/D	1.6	1.7	1.3	2.0	−0.7
μ_b/D	1.4	1.2	−1.3	0.9	0.5
μ_c/D	−0.8	-0.8	0.3	-0.5	−0.8
$\Delta E_{0,BSSE}$[b]/kJ mol^{-1}	0	0.6	2.5	4.3	4.9

[a] *A*, *B*, and *C* are rotational constants. μ_a, μ_b, and μ_c are electric dipole moments. [b] Zero-point relative energy with BSSE corrections, the absolute energies for the global minima are -653.378718 E_h.

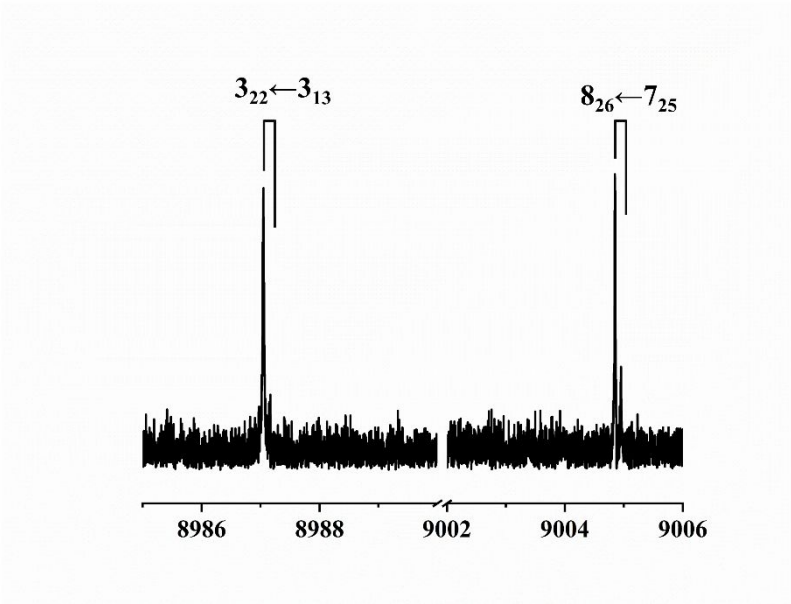

Figure S2a Section of the microwave spectrum containing μ_a-type ($8_{26} \leftarrow 7_{25}$), and μ_b-type ($3_{22} \leftarrow 3_{13}$) rotational transitions of the observed isomer phenol-CO_2. Each component exhibits an instrumental Doppler doubling.

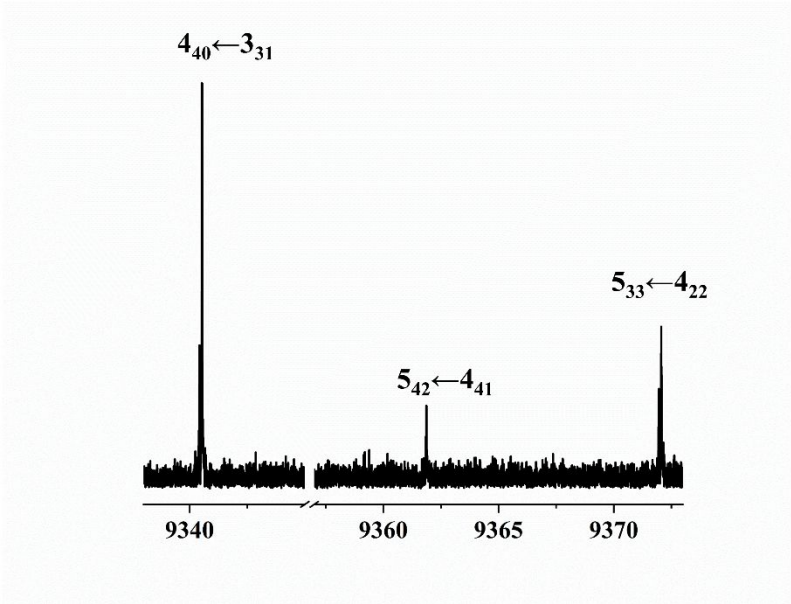

Figure S2b Section of the microwave spectrum containing μ_a-type ($5_{42} \leftarrow 4_{41}$), and μ_b-type ($4_{40} \leftarrow 3_{31}$), ($5_{33} \leftarrow 4_{22}$) rotational transitions of the observed isomer PM-CO_2. Each component exhibits an instrumental Doppler doubling.

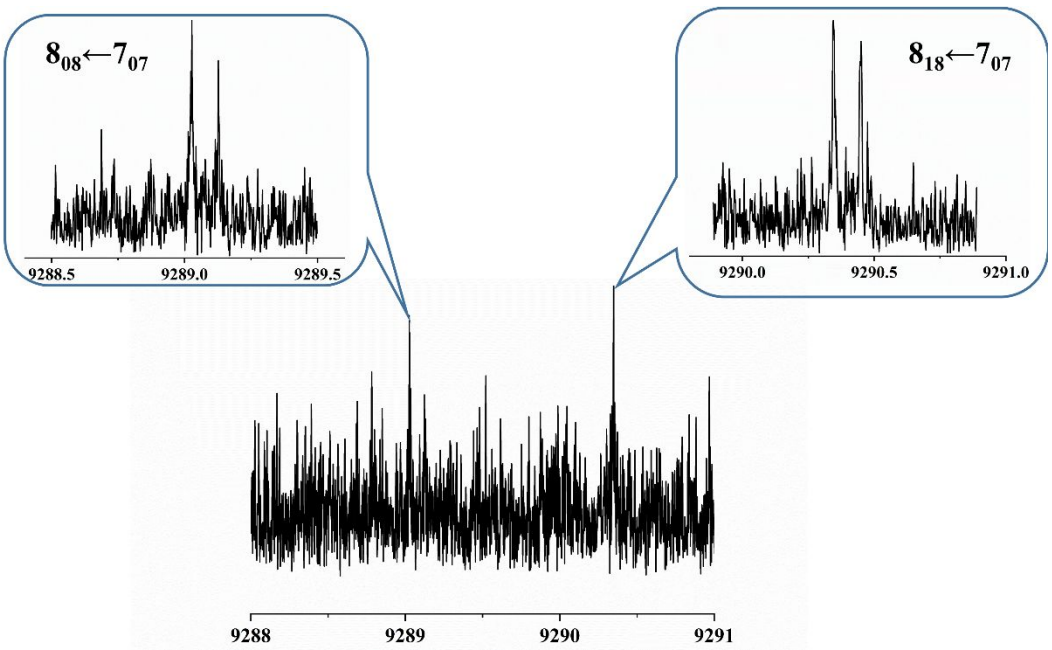

Figure S2c Section of the microwave spectrum containing μ_a-type ($8_{08} \leftarrow 7_{07}$), and μ_b-type ($8_{18} \leftarrow 7_{07}$) rotational transitions of the observed isomer 2PE-CO_2. Each component exhibits an instrumental Doppler doubling.

Table S2a. Partial r_0 and B3LYP-D3(BJ)/aug-cc-pVTZ calculated geometries of phenol-CO_2.

Bond lengths (Å)		Valence angles (°)		Dihedral angles (°)	
C1C2	1.392				
C2C3	1.393	C1C2C3	120.4		
C3C4	1.394	C2C3C4	119.6	C1C2C3C4	0.0
C4C5	1.394	C3C4C5	120.5	C2C3C4C5	0.0
C1C6	1.395	C2C1C6	119.4	C3C2C1C6	0.0
C4O7	1.373	C3C4O7	122.2	C2C3C4O7	180.0
O7H8	0.962	C4O7H8	110.1	C3C4O7H8	0.0
C3H9	1.085	C2C3H9	120.3	C1C2C3H9	180.0
C2H10	1.083	C1C2H10	120.2	C6C1C2H10	180.0
C1H11	1.082	C2C1H11	120.2	C3C2C1H11	180.0
C6H12	1.083	C1C6H12	119.9	C2C1C6H12	180.0
C5H13	1.082	C4C5H13	119.1	C3C4C5H13	180.0
O7C14	**2.84(3)**[a]	**C4O7H14**	**134(1)**	C3C4O7H14	180.0
C14O15	1.160	O7H14H15	91.3	C4O7C14O15	0.0
C14O16	1.160	O15C14O16	180.0	O7O15C14O16	180.0

[a] Error in parentheses in units of the last digit. The parameters in bold have been adjusted to reproduce the experimental values of rotational constants. Their theoretical values are 2.80 Å and 133°, respectively.

Table S2b. Partial r_0 and B3LYP-D3(BJ)/aug-cc-pVTZ calculated geometries of PM-CO_2.

Bond lengths (Å)		Valence angles (°)		Dihedral angles (°)	
C1C2	1.388				
C2C3	1.390	C1C2C3	120.0		
C3C4	1.393	C2C3C4	120.7	C1C2C3C4	-0
C4C5	1.395	C3C4C5	118.8	C2C3C4C5	0
C5C6	1.388	C4C5C6	120.4	C3C4C5C6	-0
C4C7	1.511	C3C4O7	120.5	C2C3C4C7	-178.0
C7O8	1.421	C4O7H8	113.9	C3C4O7O8	-143.1
O8H9	0.963	C7O8H9	108.0	C4C7O8H9	61.9
C7H10	1.094	C4C7H10	109.4	C3C4C7H10	-18.2
C7H11	1.091	C4C7H11	109.7	C3C4C7H11	99.1
C5H12	1.081	C4C5H12	119.0	C3C4C5H12	180.0
C6H13	1.081	C5C6H13	119.7	C4C5C6H13	180.0
C1H14	1.081	C6C1H14	120.1	C5C6C1H14	180.0
C2H15	1.081	C3C2H15	119.8	C4C3C2H15	-180.0
C3H16	1.082	C4C3H16	119.4	C5C4C3H16	-180.0
C4C17	**3.383(3)**[a]	**C3C4C17**	**84.0(3)**	C2C3C4C17	81.5
C17O18	1.163	C4C17O18	78.8	C3C4C17O18	124.5
C17O19	1.156	O18C17O19	178.6	C4O18C17O19	-174.4

[a] Error in parentheses in units of the last digit. The parameters in bold have been adjusted to reproduce the experimental values of rotational constants. Their theoretical values are 3.332 Å and 84.8°, respectively.

Table S2c. Partial r_0 and B3LYP-D3(BJ)/aug-cc-pVTZ calculated geometries of 2PE-CO_2.

Bond lengths (Å)		Valence angles (°)		Dihedral angles (°)	
C1C2	1.389				
C2C3	1.390	C1C2C3	120.1		
C3C4	1.393	C2C3C4	120.9	C1C2C3C4	-0.0
C4C5	1.396	C3C4C5	118.3	C2C3C4C5	-0.0
C5C6	1.388	C4C5C6	120.9	C3C4C5C6	0.0
C4C7	1.504	C5C4C7	120.6	C6C5C4C7	-176.9
C7O8	1.534	C4C7C8	112.3	C5C4C7C8	82.3
C8O9	1.418	C7C8O9	113.0	C4C7C8O9	63.1
O9H10	0.962	C8O9H10	108.6	C7C8O9H10	-71.9
C8H11	1.095	C7C8H11	109.6	C4C7C8H11	-60.8
C8H12	1.089	C7C8H12	109.4	C4C7C8H12	-178.9
C7H13	1.090	C4C7H13	110.1	C5C4C7H13	-156.6
C7H14	1.092	C4C7H14	110.1	C5C4C7H14	-38.2
C5H15	1.082	C6C5H15	119.6	C1C6C5H15	180.0
C6H16	1.081	C5C6H16	119.9	C4C5C6H16	-180.0
C1C17	1.081	C6C1C17	120.1	C5C6C1H17	180.0
C2H18	1.081	C3C2O18	119.7	C4C3C2H18	180.0
C3H19	1.081	C4C3O19	119.2	C5C4C3H19	-180.0
C1C20	**3.332(4)**[a]	**C6C1C20**	**80.3(2)**	C5C6C1C20	85.8
C20O21	1.160	C1C20O21	95.5	C6C1C20O21	-87.3
C20O22	1.158	O21C20O22	178.5	C1O21C20O22	170.4

[a] Error in parentheses in units of the last digit. The parameters in bold have been adjusted to reproduce the experimental values of rotational constants. Their theoretical values are 3.291 Å and 78.9°, respectively.

Table S3. SAPT analysis for $C_6H_5(CH_2)_{0\text{-}4}OH\text{-}CO_2$ complexes (all values in kJ mol^{-1}).

	Electrostatics	Induction	Dispersion	$Total_{attracting\ energy}$[a]	Exchange	Total
Phenol-CO_2	-16.8(53.3%)[b]	-2.7(8.6%)	-12.0(38.1%)	-31.5	18.2	-13.3
PM-CO_2	-16.8(40.0%)	-4.7(11.2%)	-20.5(48.8%)	-42.0	25.0	-18.4
2PE-CO_2	-16.8(39.9%)	-4.2(10.0%)	-21.1(50.1%)	-42.1	25.4	-18.4
3PP-CO_2	-26.9(47.2%)	-5.7(10.0%)	-24.4(42.8%)	-57.0	36.7	-20.3
4PB-CO2	-24.7(46.6%)	-5.0(9.4%)	-23.3(43.9)	-53.0	33.3	-19.7

[a] The sum of the three adsorption energies. [b] Percentage contribution to total attracting energy.

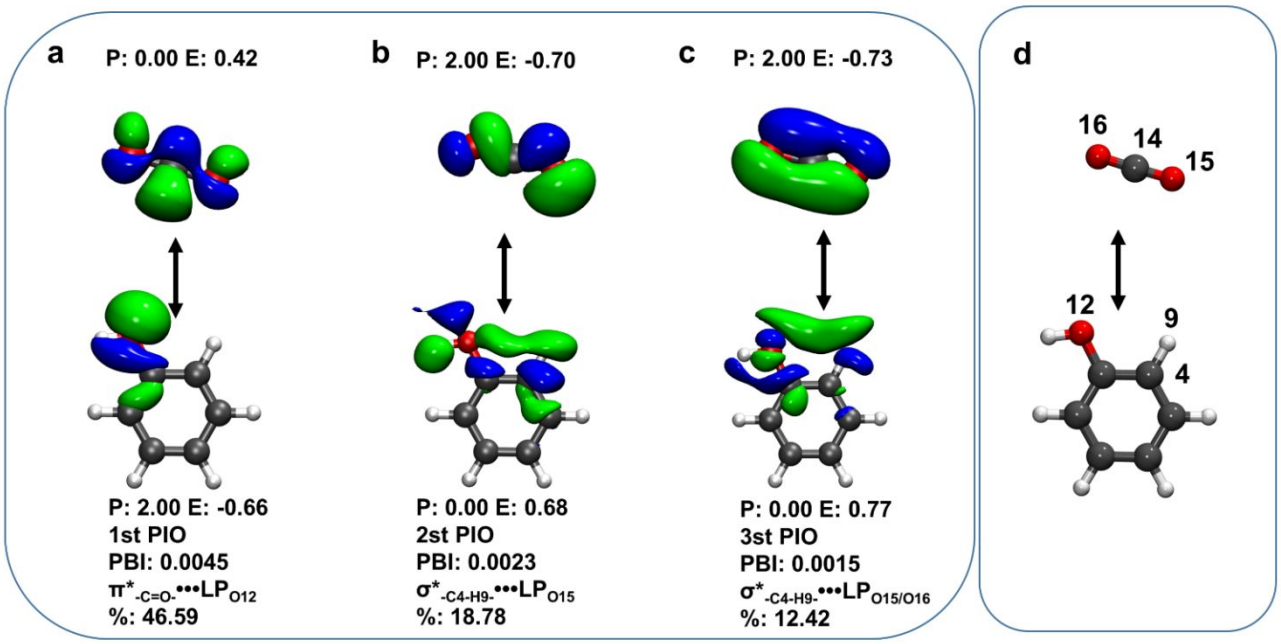

Figure S3A Results of PIO analysis on the phenol-CO_2 complex with phenol and CO_2 as two fragments based on calculations at B3LYP-D3(BJ)/aug-cc-pVTZ level of theory. a-c: The top three PIOs of each fragment. The orbital energies and populations (occupation numbers) are given as E and P, respectively, near each PIO. Given below each PIO pair are the PIO-based bond indices (abbreviated as PBI) and its contribution (as %) to the total interactions between two fragments (the contributions of all PIOs sum up to 100%). The main interactions reflected by PIO. Isovalue: 0.04 for all orbitals. d: Two fragments with phenol and CO_2.

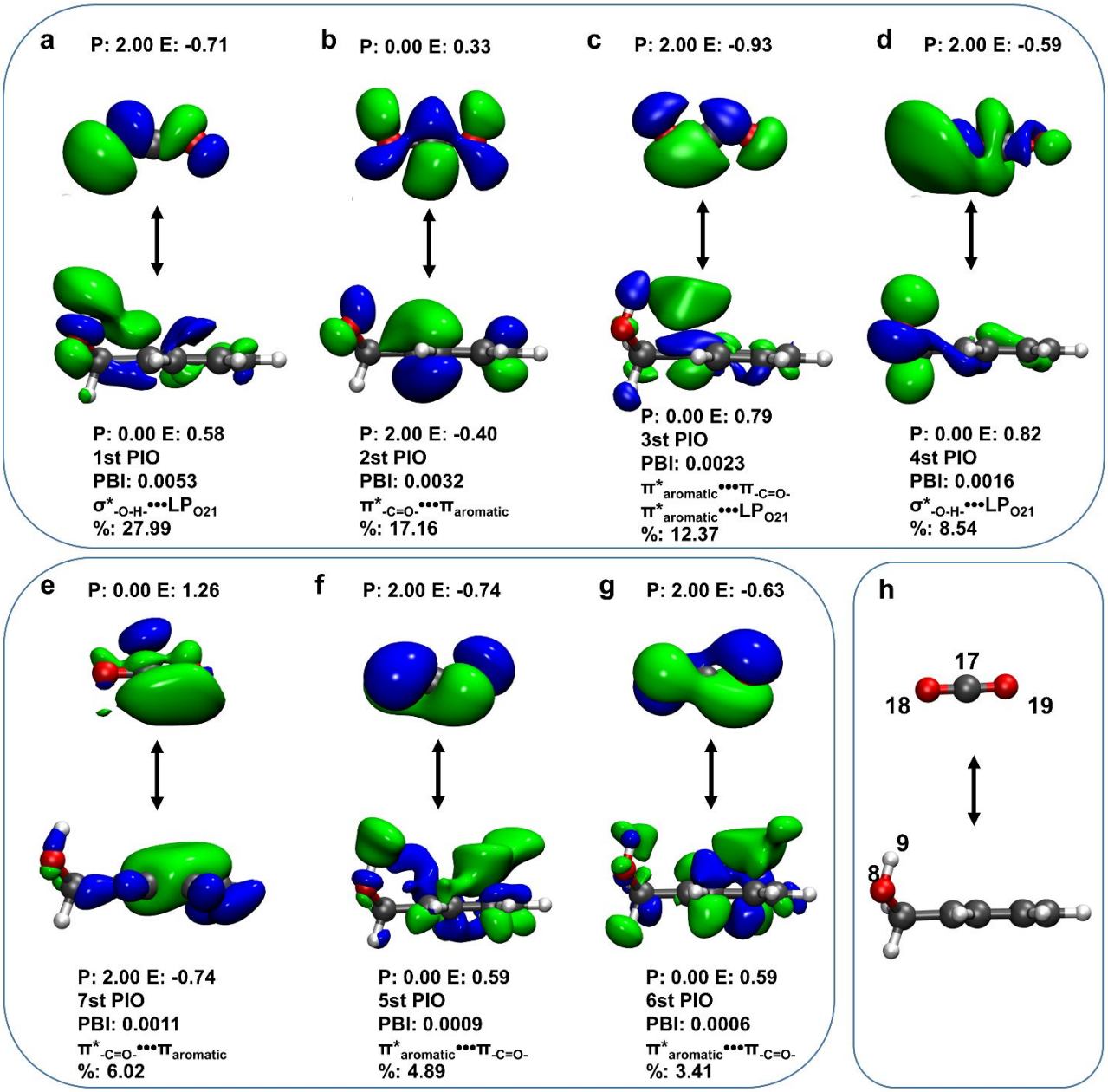

Figure S3B Results of PIO analysis on the PM-CO_2 complex with PM and CO_2 as two fragments based on calculations at B3LYP-D3(BJ)/aug-cc-pVTZ level of theory. a-g: The top seven PIOs of each fragment. The orbital energies and populations (occupation numbers) are given as E and P, respectively, near each PIO. Given below each PIO pair are the PIO-based bond indices (abbreviated as PBI) and its contribution (as %) to the total interactions between two fragments (the contributions of all PIOs sum up to 100%). The main interactions reflected by PIO. Isovalue: 0.04 for all orbitals. h: Two fragments with PM and CO_2.

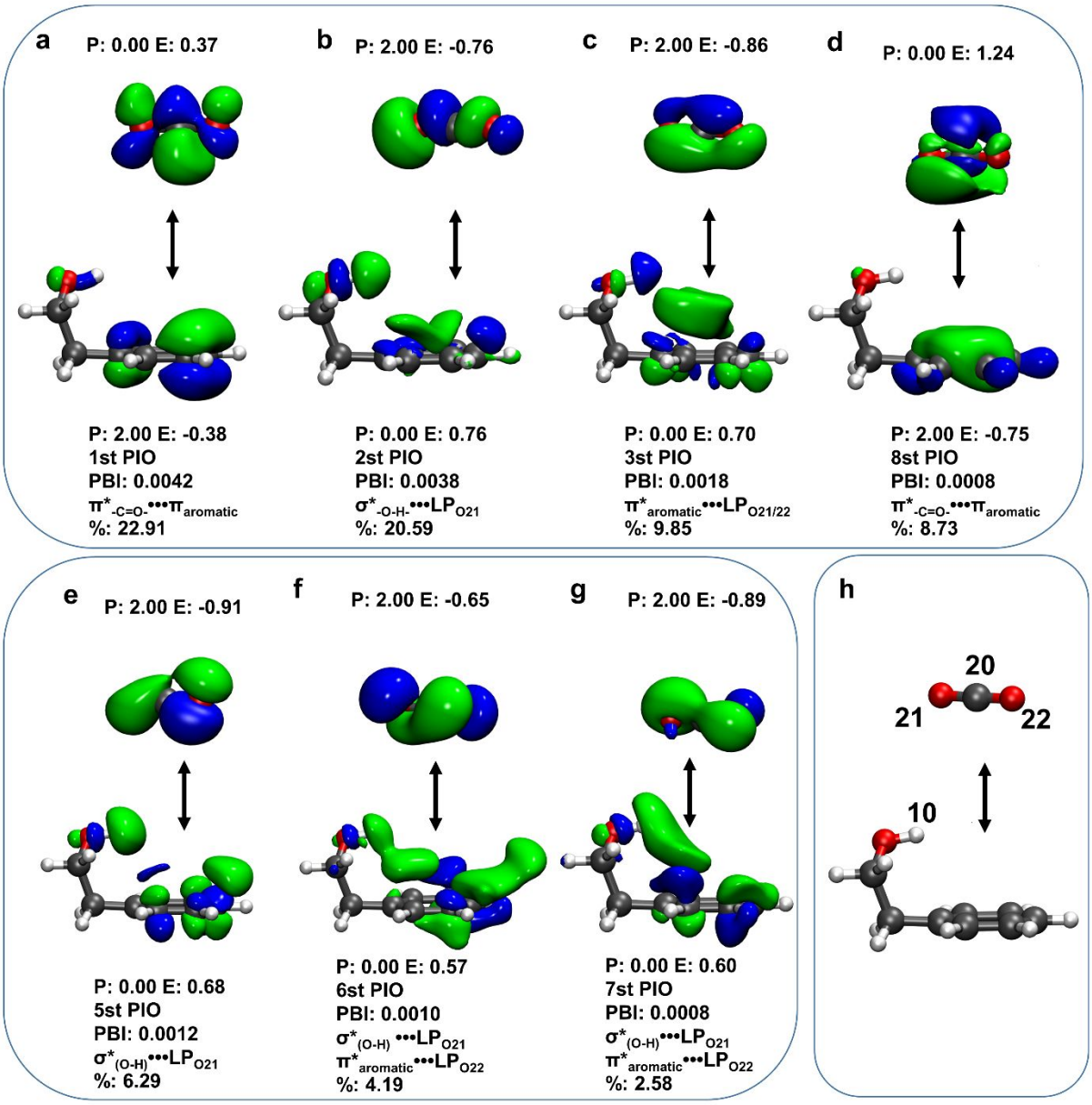

Figure S3C Results of PIO analysis on the 2PE-CO_2 complex with 2PE and CO_2 as two fragments based on calculations at B3LYP-D3(BJ)/aug-cc-pVTZ level of theory. a-g: The top seven PIOs of each fragment. The orbital energies and populations (occupation numbers) are given as E and P, respectively, near each PIO. Given below each PIO pair are the PIO-based bond indices (abbreviated as PBI) and its contribution (as %) to the total interactions between two fragments (the contributions of all PIOs sum up to 100%). The main interactions reflected by PIO. Isovalue: 0.04 for all orbitals. h: Two fragments with 2PE and CO_2.

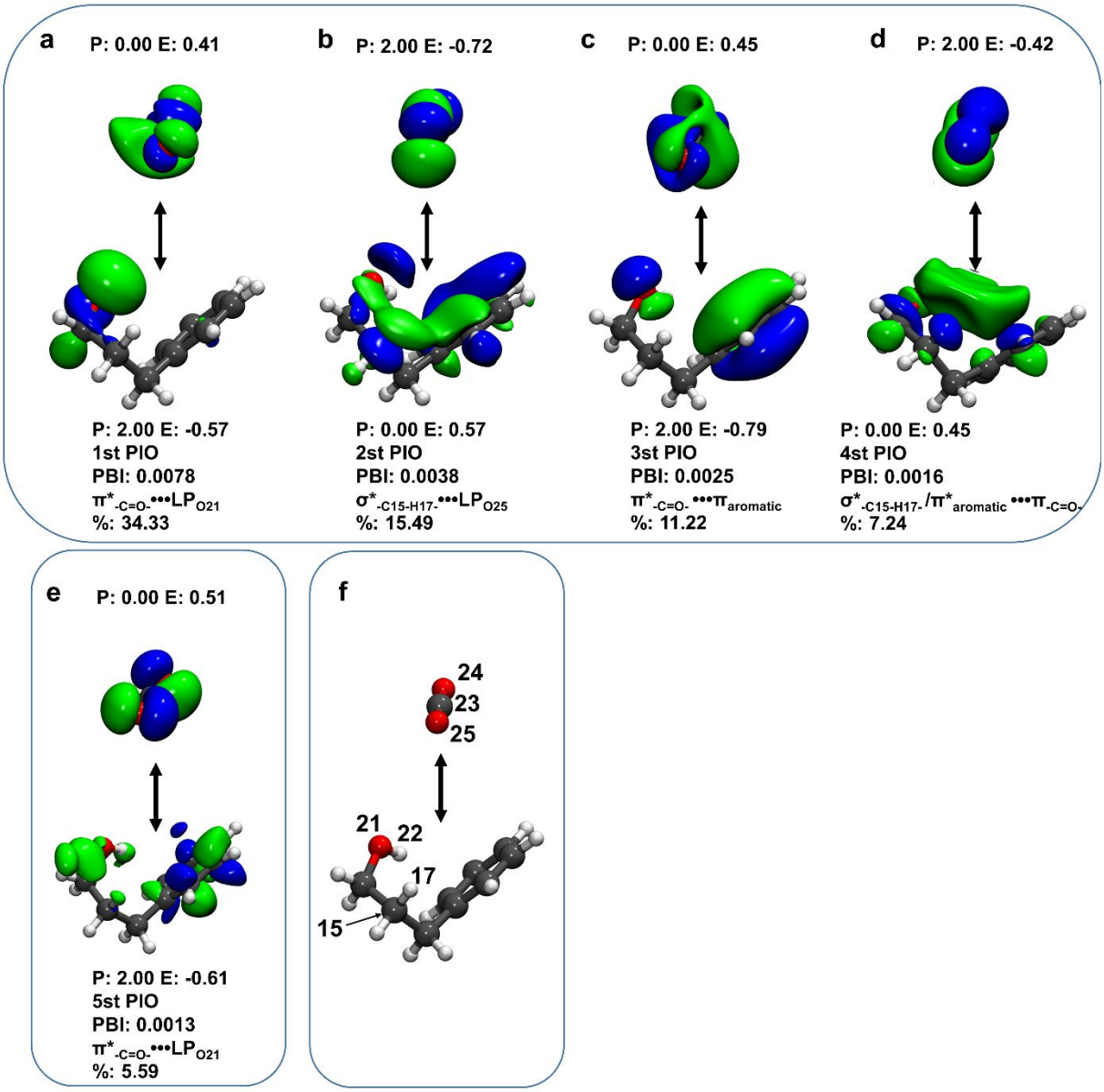

Figure S3D Results of PIO analysis on the 3PP-CO_2 complex with 3PP and CO_2 as two fragments based on calculations at B3LYP-D3(BJ)/aug-cc-pVTZ level of theory. a-e: The top five PIOs of each fragment. The orbital energies and populations (occupation numbers) are given as E and P, respectively, near each PIO. Given below each PIO pair are the PIO-based bond indices (abbreviated as PBI) and its contribution (as %) to the total interactions between two fragments (the contributions of all PIOs sum up to 100%). The main interactions reflected by PIO. Isovalue: 0.04 for all orbitals. f: Two fragments with 3PP and CO_2.

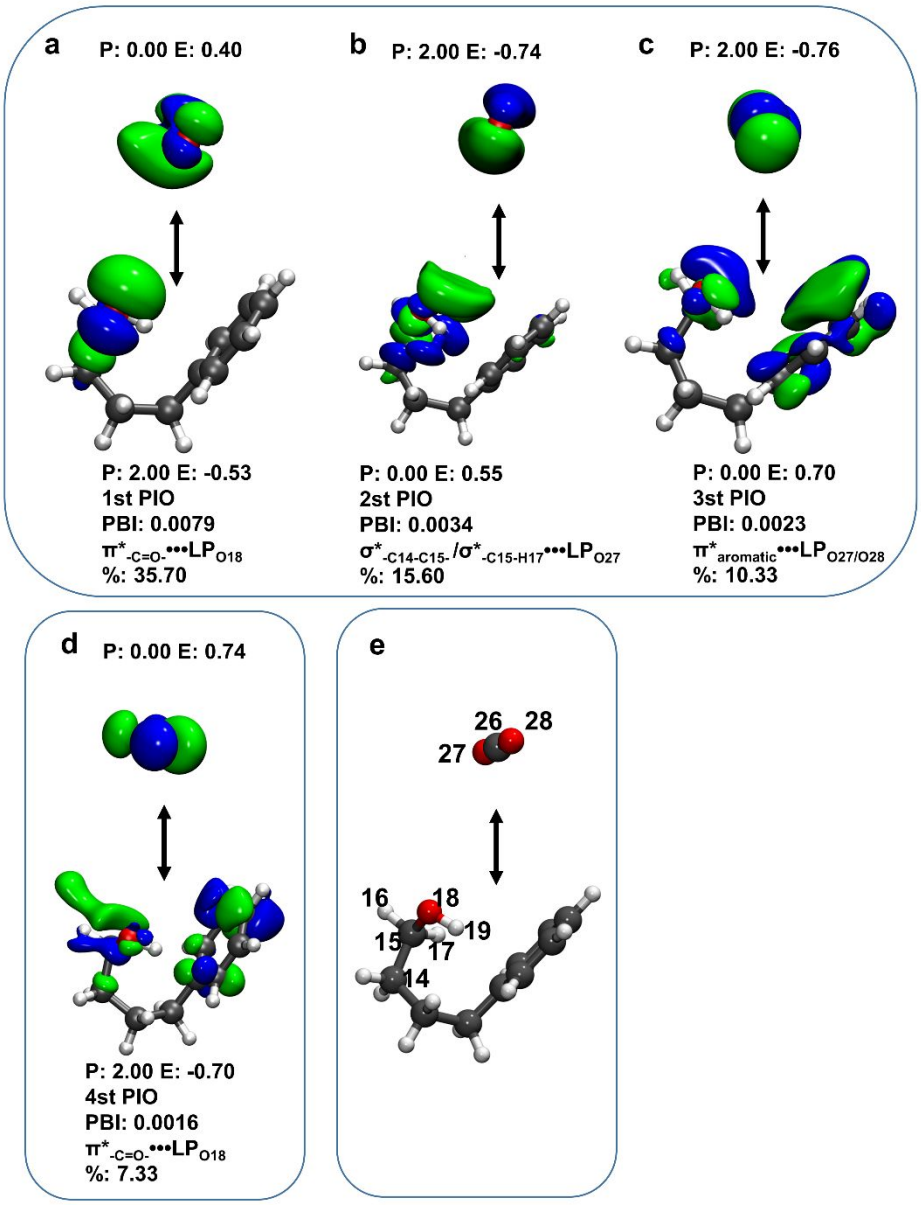

Figure S3E Results of PIO analysis on the 4PB-CO_2 complex with 4PB and CO_2 as two fragments based on calculations at B3LYP-D3(BJ)/aug-cc-pVTZ level of theory. a-d: The top four PIOs of each fragment. The orbital energies and populations (occupation numbers) are given as E and P, respectively, near each PIO. Given below each PIO pair are the PIO-based bond indices (abbreviated as PBI) and its contribution (as %) to the total interactions between two fragments (the contributions of all PIOs sum up to 100%). The main interactions reflected by PIO. Isovalue: 0.04 for all orbitals. e: Two fragments with 4PB and CO_2

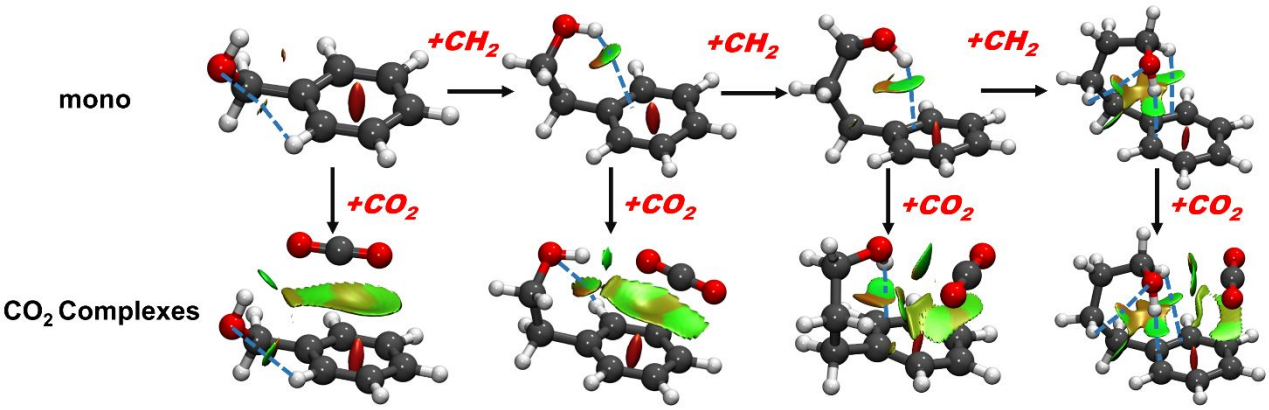

E [kJ mol^{-1}]	PM	2PE	3PP	4PB
HB	C-H···O	From O-H···π to C-H···O[b]	O-H···π	O-H···π, C-H···π and C-H···O[c]
mono	-[a]	-4.60 (O-H···π)	-8.41	-11.46/-16.44
CO_2 Complexes	-4.27	-3.35 (C-H···O)	-8.49	-12.43/-17.74

Figure S4 Intramolecular hydrogen bond analysis of the $C_6H_5(CH_2)_{1\text{-}4}OH$ monomer and $C_6H_5(CH_2)_{1\text{-}4}OH\text{-}CO_2$ complexes by AIM analysis at B3LYP-D3(BJ)/aug-cc-pVTZ level of theory. [a] The intramolecular HB of PM is weak and cannot be quantified by AIM analyses.[15] [b] After 2PE is combined with CO_2, the intramolecular hydrogen bond changes from O-H···π HB to C-H···O HB. [c] There are three intramolecular bonds O-H···π HB, C-H···π HB and C-H···O HB in the 4PB monomer and 4PB-CO_2 complexes. The red values on the left represents O-H···π HB, and the blue values on the right represents the total energy of the three molecular HBs.

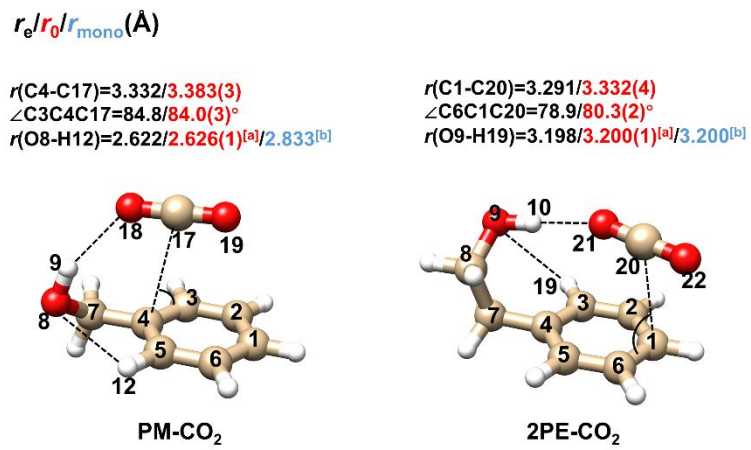

Figure S5 Structures (r_0 and r_e) of PM/2PE monomers and CO_2 clusters. [a] r_0 structures derived parameters; [b] r_{mono} (blue) is derived from the r_0 structures of PM and 2PE monomers, based on reported experimental parameters.[17,18]

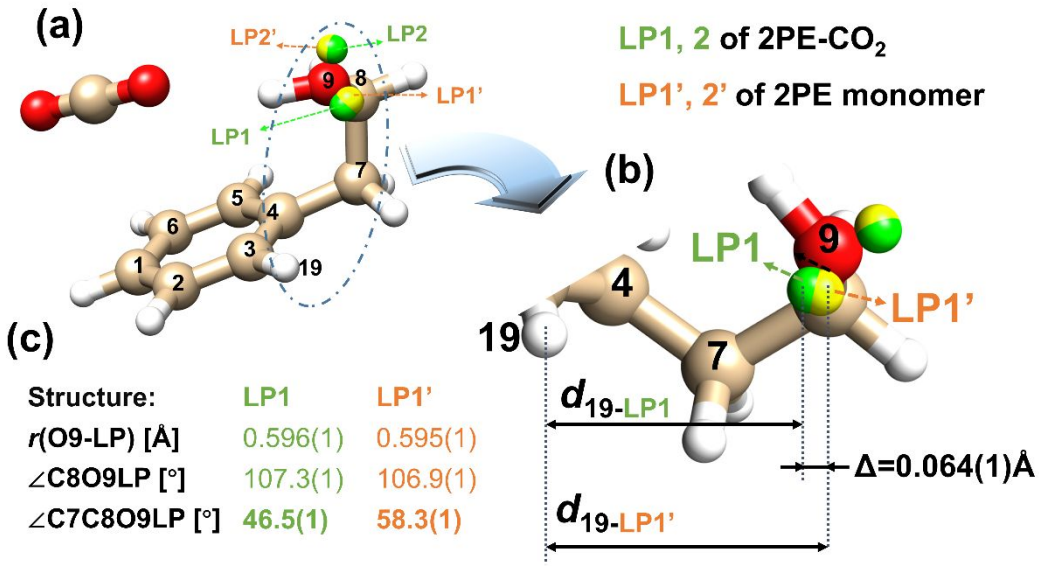

Figure S6 C3-H19···O9 intramolecular HB in 2PE-CO_2. (a) Structure of 2PE-CO_2 including LP1,2 (green ellipsoid) from the O atom of 2PE-CO_2 and LP1',2' (yellow transparent ellipsoid) from the O atom of 2PE monomer. (b) The difference Δ of the distances between H19 and LP1 ($d_{19\text{-LP1}}$), and between H19 and LP1' ($d_{19\text{-LP1'}}$). (c) Both LP positions of O9 based on electron localization function (ELF) analysis generated by the Multiwfn software, including distances (*r*), valence angles and dihedral angles.

Table S4. μ_a- and μ_b- type transition frequencies (ν/MHz) together with the corresponding observed – calculated differences ($\Delta\nu$/kHz) for the phenol-CO_2 complex.

Transitions		ν/MHz	$\Delta\nu$/kHz
J' K_a' K_c'	← J'' K_a'' K_c''		
6 1 6	5 1 5	6378.3701	-4.8
6 0 6	5 0 5	6587.0708	0.6
6 2 5	5 2 4	6645.6281	-0.9
6 3 4	5 3 3	6664.4422	0.2
6 3 3	5 3 2	6665.9752	1.4
6 2 4	5 2 3	6712.9383	1.9
6 1 5	5 1 4	6899.1308	-1.9
4 1 4	3 0 3	6914.0410	-1.3
7 1 7	6 1 6	7434.7898	4.7
7 0 7	6 0 6	7657.0804	1.8
7 2 6	6 2 5	7748.2447	-1.5
7 4 4	6 4 3	7773.2305	1.0
7 4 3	6 4 2	7773.2653	-2.4
7 3 5	6 3 4	7778.0192	-0.4
7 3 4	6 3 3	7781.4592	0.3
5 1 5	4 0 4	7816.6857	-0.5
7 1 6	6 1 5	8040.6678	2.0
5 2 3	5 1 4	8148.0948	1.1
4 2 2	4 1 3	8322.4267	2.0
3 2 1	3 1 2	8474.5652	0.8
8 1 8	7 1 7	8488.4805	1.0
6 1 6	5 0 5	8688.4817	-1.1
8 0 8	7 0 7	8715.9364	-2.7
8 2 7	7 2 6	8848.5753	1.1
8 4 5	7 4 4	8886.1921	1.4
8 4 4	7 4 3	8886.2917	-3.9
8 3 6	7 3 5	8892.5551	2.7
8 3 5	7 3 4	8899.4096	0.9
3 2 2	3 1 3	8987.0935	-4.5
8 2 6	7 2 5	9004.8992	-0.4
8 1 7	7 1 6	9177.9657	0.6
5 2 4	5 1 5	9385.0888	0.0
7 1 7	6 0 6	9536.1943	-3.4
9 1 9	8 1 8	9539.3064	0.2
6 2 5	6 1 6	9652.3444	1.5

9 0 9	8 0 8	9763.7087	1.7
9 2 8	8 2 7	9946.3000	-0.6
9 4 6	8 4 5	10000.1286	0.7
9 4 5	8 4 4	10000.3776	-1.9
9 3 7	8 3 6	10007.9409	0.0
9 3 6	8 3 5	10020.4506	-1.3
9 2 7	8 2 6	10163.6570	0.9
9 1 8	8 1 7	10310.1480	-0.5
8 2 7	8 1 8	10325.8954	-3.4
8 1 8	7 0 7	10367.5975	-1.0
10 1 10	9 1 9	10587.1890	-0.6
10 0 10	9 0 9	10801.2114	1.2
2 2 1	1 1 0	10899.3659	0.9
2 2 0	1 1 1	10988.3736	-0.3
10 2 9	9 2 8	11041.1279	3.5
10 4 7	9 4 6	11115.1403	1.1
10 4 6	9 4 5	11115.6843	0.7
10 3 8	9 3 7	11124.0082	-1.2
10 3 7	9 3 6	11145.3156	0.0
9 1 9	8 0 8	11190.9635	-2.0
10 1 9	9 1 8	11436.2357	0.3
11 1 11	10 1 10	11632.1299	0.7
11 0 11	10 0 10	11829.9498	-2.4
3 2 2	2 1 1	11921.3973	-0.5
11 2 10	10 2 9	12132.7600	0.4
3 2 1	2 1 2	12192.3246	-0.5
11 1 10	10 1 9	12555.1497	-0.8
12 1 12	11 1 11	12674.1933	1.0
12 0 12	11 0 11	12851.8706	-0.2
4 2 3	3 1 2	12899.6124	0.5
12 3 10	11 3 9	13357.1155	-2.0
4 2 2	3 1 3	13451.1532	1.2
12 1 11	11 1 10	13665.7487	0.7
13 1 13	12 1 12	13713.5054	-0.8
5 2 4	4 1 3	13834.2251	1.1
13 0 13	12 0 12	13869.0225	-0.4
7 3 4	7 2 5	14371.1084	0.2
6 3 3	6 2 4	14444.1727	0.7
5 3 2	5 2 3	14491.1352	0.6

4 3 1	4 2 2	14518.5374	-0.3
4 3 2	4 2 3	14547.5894	0.4
5 3 3	5 2 4	14558.3881	-2.2
6 3 4	6 2 5	14577.2043	1.0
7 3 5	7 2 6	14606.9778	1.2
6 2 5	5 1 4	14725.7014	1.4
5 2 3	4 1 4	14772.5878	-0.1
14 0 14	13 0 13	14883.2934	-2.1
7 2 6	6 1 5	15574.8141	0.6
15 0 15	14 0 14	15896.2195	2.1
6 2 4	5 1 5	16166.0487	0.7
8 2 7	7 1 6	16382.7217	-0.1
9 2 8	8 1 7	17151.0589	1.4
7 2 5	6 1 6	17642.1962	0.6
3 3 1	2 2 0	17867.5268	-1.5
3 3 0	2 2 1	17869.5085	-1.2

Table S5. μ_a-, μ_b- and μ_c- type transition frequencies (ν/MHz) together with the corresponding observed – calculated differences ($\Delta\nu$/kHz) for the PM-CO_2 complex.

Transitions		ν/MHz	$\Delta\nu$/kHz
J' K_a' K_c'	← J'' K_a'' K_c''		
3 2 2	2 2 1	5302.9894	3.7
3 2 1	2 2 0	5922.4357	-4.3
4 0 4	3 1 3	6090.1977	-1.1
4 1 4	3 1 3	6090.7241	-0.9
4 0 4	3 0 3	6094.5133	0.0
4 1 4	3 0 3	6095.0410	1.5
3 3 1	2 2 0	6682.1109	2.2
4 1 3	3 2 2	6822.4316	2.4
4 2 3	3 2 2	6851.6680	0.1
4 1 3	3 1 2	6959.4718	0.0
4 2 3	3 1 2	6988.7095	-1.0
3 3 0	2 2 1	7077.5554	-1.9
4 3 2	3 3 1	7359.0526	-1.4
3 3 0	2 1 1	7459.5811	5.5
5 0 5	4 1 4	7514.0096	1.2
5 1 5	4 1 4	7514.0658	-0.4
5 0 5	4 0 4	7514.5345	0.0
5 1 5	4 0 4	7514.5914	-1.0
4 2 2	3 2 1	7752.3294	-0.2
4 3 1	3 3 0	7873.1616	-1.1
4 3 2	3 2 1	8118.7253	2.6
5 1 4	4 2 3	8309.8015	-0.2
5 2 4	4 2 3	8314.4381	0.5
5 1 4	4 1 3	8339.0406	0.1
5 2 4	4 1 3	8343.6771	0.8
6 0 6	5 1 5	8936.0467	-5.8
6 1 6	5 1 5	8936.0602	1.6
6 0 6	5 0 5	8936.1090	-1.5
6 1 6	5 0 5	8936.1215	5.0
5 3 3	4 3 2	9005.6166	0.0
4 4 1	3 3 0	9117.1098	-0.9
5 2 3	4 2 2	9262.5586	-0.4
4 4 0	3 3 1	9340.4815	-1.8
5 4 2	4 4 1	9361.8193	1.9

5 3 3	4 2 2	9372.0090	-0.5
5 4 1	4 4 0	9737.4395	0.2
6 1 5	5 2 4	9743.9816	-0.1
6 2 5	5 2 4	9744.6086	0.4
6 1 5	5 1 4	9748.6164	-1.1
6 2 5	5 1 4	9749.2448	0.9
4 3 1	3 1 2	9784.7769	-0.2
5 3 2	4 3 1	9874.7420	1.4
7 1 7	6 1 6	10357.8753	-1.9
7 0 7	6 1 6	10357.8753	-1.3
7 0 7	6 0 6	10357.8854	2.8
7 1 7	6 0 6	10357.8854	2.2
6 2 4	5 3 3	10502.3720	0.0
6 3 4	5 3 3	10524.6905	0.3
5 4 2	4 3 1	10605.7625	-2.8
6 2 4	5 2 3	10611.8230	0.5
6 3 4	5 2 3	10634.1406	-0.1
5 3 2	4 2 2	10903.1264	0.1
5 4 1	4 3 1	11056.8752	-0.5
6 4 3	5 4 2	11111.3432	0.1
7 1 6	6 2 5	11167.2397	1.4
7 2 6	6 2 5	11167.3148	0.0
7 1 6	6 1 5	11167.8646	0.0
7 2 6	6 1 5	11167.9414	0.1
5 4 2	4 3 2	11267.7578	-0.3
6 5 2	5 5 1	11319.0697	-2.6
5 5 1	4 4 0	11537.4886	-0.1
6 3 3	5 3 2	11550.2081	-0.2
6 5 1	5 5 0	11555.2368	0.7
5 5 0	4 4 0	11571.9439	-0.2
5 5 1	4 4 1	11612.9774	0.0
5 5 0	4 4 1	11647.4324	-0.3
5 4 1	4 3 2	11718.8664	-2.1
8 0 8	7 0 7	11779.6564	-0.2
8 1 8	7 1 7	11779.6564	0.2
8 0 8	7 1 7	11779.6564	0.3
8 1 8	7 0 7	11779.6564	-0.3
6 4 3	5 3 2	11842.3665	-1.4
6 4 2	5 4 1	11899.2557	-0.2

7 2 5	6 3 4	11970.1524	-1.2
7 3 5	6 3 4	11973.8114	-0.5
7 2 5	6 2 4	11992.4722	0.2
7 3 5	6 2 4	11996.1294	-0.7
5 4 1	4 2 2	12085.2635	1.9
8 1 7	7 2 6	12588.8882	-6.0
8 2 7	7 2 6	12588.9050	2.0
8 1 7	7 1 6	12588.9679	-2.9
8 2 7	7 1 6	12588.9835	3.9
7 4 4	6 4 3	12709.9587	0.4
7 3 4	6 3 3	12925.3281	-0.2
7 4 4	6 3 3	13002.1174	-0.4
6 4 2	5 3 2	13081.3906	-0.5
6 5 2	5 4 1	13119.1212	-0.6
7 5 3	6 5 2	13164.4859	0.8
6 3 3	5 2 3	13190.7767	1.1
9 0 9	8 0 8	13201.3998	-0.2
9 1 9	8 1 8	13201.3998	-0.1
9 0 9	8 1 8	13201.3998	-0.1
9 1 9	8 0 8	13201.3998	-0.2
7 6 2	6 6 1	13241.7380	1.4
7 6 1	6 6 0	13371.2708	0.0
6 4 3	5 3 3	13373.4847	0.0
6 5 1	5 4 1	13389.7403	-0.6
8 2 6	7 3 5	13399.3487	-0.4
8 3 6	7 3 5	13399.8751	1.4
8 2 6	7 2 5	13403.0067	-0.7
8 3 6	7 2 5	13403.5307	-1.2
6 5 2	5 4 2	13570.2299	-2.3
7 4 3	6 4 2	13770.7809	0.2
7 5 2	6 5 1	13816.9863	-1.0
6 5 1	5 4 2	13840.8526	1.2
6 6 1	5 5 0	13935.4585	0.2
6 6 0	5 5 0	13950.0787	0.3
6 6 1	5 5 1	13969.9142	0.5
6 6 0	5 5 1	13984.5321	-1.6
9 2 8	8 2 7	14010.4006	-1.4
9 1 8	8 2 7	14010.4006	-0.4
9 1 8	8 1 7	14010.4126	2.8

9 2 8	8 1 7	14010.4126	1.8
8 4 5	7 4 4	14197.2034	0.7
8 3 5	7 3 4	14258.7801	1.0
7 5 3	6 4 2	14384.3517	0.6
6 5 1	5 3 2	14571.8786	2.3
10 0 10	9 0 9	14623.1025	0.6
10 1 10	9 1 9	14623.1025	0.6
10 0 10	9 1 9	14623.1025	0.6
10 1 10	9 0 9	14623.1025	0.6
6 4 2	5 2 3	14721.9600	1.5
9 3 7	8 3 6	14821.2168	0.7
9 2 7	8 2 6	14821.6726	0.5
8 5 4	7 5 3	14857.9299	0.5
8 6 3	7 6 2	15166.1503	1.7
8 4 4	7 4 3	15263.5801	0.0
10 1 9	9 1 8	15431.9039	-0.8
10 2 9	9 2 8	15431.9039	0.0
7 6 2	6 5 1	15621.9598	0.9
9 4 6	8 4 5	15633.6247	1.3
8 6 2	7 6 1	15644.5887	0.0
9 3 6	8 3 5	15646.2936	-0.8
8 5 3	7 5 2	15891.2209	1.1
7 6 1	6 5 2	16036.7293	-2.8
11 0 11	10 0 10	16044.7547	-0.5
11 1 11	10 1 10	16044.7547	-0.5
11 1 11	10 0 10	16044.7547	-0.5
11 0 11	10 1 10	16044.7547	-0.5
10 3 8	9 3 7	16242.0798	3.9
10 2 8	9 2 7	16242.1325	-3.5
7 7 1	6 6 0	16317.4735	1.1
7 7 0	6 6 1	16337.9996	-2.0
9 5 5	8 5 4	16406.1733	0.0
9 4 5	8 4 4	16564.0116	-2.2
7 5 2	6 3 3	16838.6547	-0.5
11 1 10	10 1 9	16853.3896	0.0
11 2 10	10 2 9	16853.3896	0.0
9 6 4	8 6 3	16958.7973	0.6
10 4 7	9 4 6	17055.7141	0.0
10 3 7	9 3 6	17057.8774	0.0

9 5 4	8 5 3	17575.8216	-1.9
9 6 3	8 6 2	17894.5876	-0.5
8 7 2	7 6 1	18087.4808	0.6
8 7 1	7 6 2	18301.6077	-0.3
8 8 1	7 7 0	18690.9230	0.5
8 8 0	7 7 1	18699.1409	1.4

Table S6. μ_a-, μ_b- and μ_c- type transition frequencies (ν/MHz) together with the corresponding observed – calculated differences ($\Delta\nu$/kHz) for the 2PE-CO_2 complex.

Transitions		ν/MHz	$\Delta\nu$/kHz
J' K_a' K_c'	← J'' K_a'' K_c''		
5 0 5	4 1 4	5883.3823	0.0
5 1 5	4 0 4	5978.6951	-0.2
4 2 3	3 1 2	6163.1293	2.1
3 3 1	2 2 0	6395.4929	-2.1
3 3 0	2 2 0	6404.2301	-4.9
5 2 4	4 2 3	6410.2391	0.4
3 3 1	2 2 1	6445.1799	-1.5
3 3 0	2 2 1	6453.9234	1.9
5 1 4	4 1 3	6678.6257	-2.0
4 2 2	3 1 2	6757.0688	1.8
5 2 3	4 2 2	6969.3080	0.7
6 0 6	5 1 5	7030.9286	-1.2
6 1 6	5 1 5	7041.3861	1.5
6 0 6	5 0 5	7058.5089	0.4
6 1 6	5 0 5	7068.9648	1.6
5 2 4	4 1 3	7116.7407	-1.3
6 1 5	5 2 4	7377.1112	-3.6
4 3 2	3 2 1	7599.2041	1.6
6 2 5	5 2 4	7610.7711	-1.4
4 3 1	3 2 1	7657.6364	0.4
6 1 5	5 1 4	7815.2292	0.0
4 3 2	3 2 2	7827.7337	0.8
4 3 1	3 2 2	7886.1672	0.8
6 3 4	5 3 3	7925.2259	0.0
6 2 5	5 1 4	8048.8887	1.8
7 0 7	6 1 6	8161.6793	-0.2
7 0 7	6 0 6	8172.1329	-1.4
7 1 7	6 0 6	8175.9128	-1.1
6 3 3	5 3 2	8256.3020	-1.6
5 2 3	4 1 3	8269.7507	0.2
7 2 5	6 3 4	8315.9706	-1.0
6 2 4	5 2 3	8334.7871	-1.2
5 1 4	4 0 4	8532.2826	1.3
7 1 6	6 2 5	8671.5429	-0.1

5 3 3	4 2 2	8676.9383	5.1
4 4 1	3 3 0	8726.2041	1.1
4 4 0	3 3 0	8727.4688	-0.8
4 4 1	3 3 1	8734.9428	-0.1
4 4 0	3 3 1	8736.2084	-1.1
7 2 6	6 2 5	8781.3983	1.8
5 3 2	4 2 2	8889.6756	0.8
5 2 4	4 1 4	8902.6599	-1.2
7 1 6	6 1 5	8905.1970	-3.8
7 2 6	6 1 5	9015.0554	1.1
7 3 5	6 3 4	9200.2484	2.7
5 3 3	4 2 3	9270.8738	0.8
8 0 8	7 1 7	9285.2959	-0.9
8 1 8	7 1 7	9286.6182	0.3
8 0 8	7 0 7	9289.0770	0.6
8 1 8	7 0 7	9290.3973	-0.2
5 3 2	4 2 3	9483.6172	2.6
7 2 5	6 2 4	9614.0358	0.7
6 3 4	5 2 3	9632.8491	-2.6
7 3 4	6 3 3	9742.9084	-1.9
8 1 7	7 2 6	9882.0109	-1.3
8 2 6	7 3 5	9908.7487	-0.8
6 2 4	5 1 4	9925.9094	-1.6
8 2 7	7 2 6	9929.2054	1.1
8 1 7	7 1 6	9991.8685	2.7
5 4 2	4 3 1	10011.6051	0.7
5 4 1	4 3 1	10022.6697	-0.4
8 2 7	7 1 6	10039.0574	-0.2
5 4 2	4 3 2	10070.0371	-0.8
5 4 1	4 3 2	10081.1043	0.5
6 3 3	5 2 3	10176.6706	-0.5
6 1 5	5 0 5	10396.3963	2.6
9 0 9	8 1 8	10406.1205	1.7
9 1 9	8 1 8	10406.5693	0.2
9 0 9	8 0 8	10407.4398	0.0
9 1 9	8 0 8	10407.8882	-1.9
8 3 6	7 3 5	10438.9036	-0.9
7 3 5	6 2 4	10498.3110	1.9
6 2 5	5 1 5	10602.4722	-0.5

6 3 4	5 2 4	10785.8576	-2.5
8 2 6	7 2 5	10793.0232	-0.3
5 5 1	4 4 0	11036.7270	1.2
5 5 0	4 4 0	11036.8910	-0.3
5 5 1	4 4 1	11037.9940	1.6
5 5 0	4 4 1	11038.1575	-0.5
9 1 8	8 2 7	11043.2884	-2.0
9 2 8	8 2 7	11062.3345	0.1
9 1 8	8 1 7	11090.4825	0.1
9 2 8	8 1 7	11109.5295	3.1
8 3 5	7 3 4	11177.1439	-1.8
6 4 3	5 3 2	11217.9221	-1.8
6 4 2	5 3 2	11270.3436	-0.2
8 3 6	7 2 5	11323.1805	1.9
6 3 3	5 2 4	11329.6811	1.5
9 2 7	8 3 6	11360.6556	4.7
6 4 3	5 3 3	11430.6649	-0.7
6 4 2	5 3 3	11483.0828	-2.7
10 0 10	9 1 9	11525.8985	1.5
10 1 10	9 1 9	11526.0451	-2.2
10 0 10	9 0 9	11526.3492	2.0
10 1 10	9 0 9	11526.5008	3.1
7 3 4	6 2 4	11584.7926	-0.5
9 3 7	8 3 6	11640.9049	2.4
7 2 5	6 1 5	11724.7165	-0.5
9 2 7	8 2 6	11890.8050	-0.9
9 3 7	8 2 6	12171.0558	-1.7
10 1 9	9 2 8	12180.0454	-2.5
10 1 9	9 1 8	12199.0914	-0.4
10 2 9	9 1 8	12206.4383	0.7
7 1 6	6 0 6	12243.0867	0.6
7 4 4	6 3 3	12291.7612	0.9
6 5 2	5 4 1	12348.9694	-2.7
6 5 1	5 4 1	12350.7527	0.0
6 5 2	5 4 2	12360.0393	1.3
6 5 1	5 4 2	12361.8193	0.8
7 3 5	6 2 5	12375.3303	-2.9
7 4 3	6 3 3	12466.9355	-0.9
9 3 6	8 3 5	12523.8974	0.6

11 0 11	10 1 10	12645.2828	-3.4
11 1 11	10 1 10	12645.3349	-0.8
11 0 11	10 0 10	12645.4382	1.4
11 1 11	10 0 10	12645.4874	1.1
7 4 4	6 3 4	12835.5800	0.2
7 4 3	6 3 4	13010.7554	-0.4
10 3 8	9 2 7	13091.4830	1.4
8 3 5	7 2 5	13147.9030	-0.8
8 4 5	7 3 4	13215.4707	-7.6
11 1 10	10 2 9	13305.8460	1.5
11 1 10	10 1 9	13313.1868	-3.3
11 2 10	10 1 9	13315.9302	2.1
6 6 1	5 5 0	13343.1812	1.8
6 6 0	5 5 0	13343.1989	-0.8
6 6 1	5 5 1	13343.3437	-1.3
6 6 0	5 5 1	13343.3634	-1.9
7 5 3	6 4 2	13634.2368	3.4
7 5 2	6 4 2	13644.5234	1.4
8 4 4	7 3 4	13667.8427	1.0
7 5 3	6 4 3	13686.6526	-0.6
7 5 2	6 4 3	13696.9435	1.6
12 0 12	11 1 11	13764.5161	0.3
12 1 12	11 1 11	13764.5341	2.2
12 0 12	11 0 11	13764.5611	-4.1
12 1 12	11 0 11	13764.5831	1.7
8 3 6	7 2 6	14032.8424	1.0
8 4 5	7 3 5	14301.9641	1.6
12 1 11	11 1 10	14429.8646	-2.1
7 6 2	6 5 1	14661.4460	-0.3
7 6 1	6 5 1	14661.7051	-0.3
7 6 2	6 5 2	14663.2275	0.6
7 6 1	6 5 2	14663.4863	0.3
8 5 3	7 4 3	14894.8200	3.3
8 5 4	7 4 4	15027.9476	-1.9

References

(1) Balle, T. J.; Flygare, W. H. Fabry-Perot Cavity Pulsed Fourier Transform Microwave Spectrometer with a Pulsed Nozzle Particle Source. *Rev. Sci. Instrum.* **1981**, *52*, 33−45.

(2) Grabow, J. U.; Stahl, W.; Dreizler, H. A Multioctave Coaxially Oriented Beam-Resonator Arrangement Fourier-transform Microwave Spectrometer. *Rev. Sci. Instrum.* **1996**, *67*, 4072−4084.

(3) Grabow, J. U.; Gou, Q; Feng, G. F. A Highly-Integrated Supersonic-Jet Fourier Transform Microwave Spectrometer, in *72nd International Symposium on Molecular Spectroscopy*, Champaign-Urbana, **2017**, TH03, P1.

(4) Frisch, M. J.; Trucks, G. W.; Schlegel, H. B.; Scuseria, G. E.; Robb, M. A.; Cheeseman, J. R.; Scalmani, G.; Barone, V.; Petersson, G. A.; Nakatsuji, H. et al. *Gaussian 16*, Rev. A.03; Gaussian, Inc.: Wallingford, CT, **2016**.

(5) Boys, S. F.; Bernardi, F. The Calculation of Small Molecular Interactions by the Differences of Separate Total Energies. Some Procedures with Reduced Errors. *Mol. Phys.* **1970**, *19*, 553−566.

(6) Pickett, H. M. The Fitting and Prediction of Vibration-Rotation Spectra with Spin Interactions. *J. Mol. Spectrosc.* **1991**, *148*, 371−377.

(7) Watson, J. K. G. In *Vibrational Spectra and Structure*; Durig, J. R., Ed.; Elsevier: New York, **1977**; Vol. 6, p1.

(8) Kisiel, Z. Spectroscopy from Space; Demaison, J., Ed.; Kluwer Academic Publishers: Dordrecht, The Netherlands, **2001**.

(9) Johnson, E. R.; Keinan, S.; Mori-Sánchez, P.; Contreras-García, J.; Cohen, A. J.; Yang, W. Revealing Noncovalent Interactions. *J. Am. Chem. Soc.* **2010**, *132*, 6498−6506.

(10) Lu, T.; Chen, F. Multiwfn: A Multifunctional Wavefunction Analyzer. *J. Comput. Chem.* **2012**, *33*, 580–592.

(11) Humphrey, W.; Dalke, A.; Schulten, K. VMD – Visual Molecular Dynamics *J. Molec. Graphics*, **1996**, *14*, 33-38.

(12) Zhang, J. X.; Sheong, F. K.; Lin, Z. Y. Unravelling Chemical Interactions with Principal Interacting Orbital Analysis. *Chem. Eur. J.* **2018**, *24*, 9639−9650.

(13) Jeziorski, B.; Moszynski, R.; Szalewicz, K. Perturbation Theory Approach to Intermolecular Potential Energy Surfaces of van der Waals Complexes. *Chem. Rev.* **1994**, *94*, 1887−1930.

(14) Parrish, R. M.; L. Burns, A.; Smith, D. G. A.; Simmonett, A. C.; DePrince III, A. E.; Hohenstein, E. G.; Bozkaya, U.; Richard, R. M.; Gonthier, J. F.; James, A. M. et al. Psi4 1.1: an Open-Source Electronic Structure Program Emphasizing Automation, Advanced Libraries, and Interoperability. *J. Chem. Theory. Comput.*, **2017**, *13*, 3185-3197.

(15) Lu, T.; Kruse, H.; Emamian, H. Exploring Nature and Predicting Strength of Hydrogen Bonds: A Correlation Analysis Between Atoms-in-Molecules Descriptors, Binding Energies, and Energy Components of Symmetry-Adapted Perturbation Theory. *J. Comput. Chem.* **2019**, *40*, 2868–2881.

(16) Maris, A.; Ottaviani, P.; Giuliano, B. M.; Melandri, S.; Caminati W. Broad Band Free Jet Absorption mm-wave Spectrum of 3-phenyl-1-propanol *J. Mol. Spectrosc.*, **2012**, *280*, 145-149.

(17) Utzat, K. A.; Bohn, R. K.; Montgomery, J. A., Jr.; Michels, H. H.; Caminati, W. Rotational Spectrum, Tunneling Motions, and Potential Barriers of Benzyl Alcohol. *J. Phys. Chem. A* **2010**, *114*, 6913–6916.

(18) Brown, R. D.; Godfrey, P. D. Detection of a Higher Energy Conformer of 2-Phenylethanol by Millimeter-Wave Spectroscopy. *J. Phys. Chem. A* **2000**, *104*, 5742–5746.

Author Contributions

Hao Wang: investigation (equal), data curation (equal), formal analysis (equal), validation (equal), writing of original draft(equal)

Junhua Chen: data curation (equal), formal analysis (equal), validation (equal), writing of original draft(equal)

Yang Zheng: data curation (equal), formal analysis (equal), validation (equal), writing of original draft(equal)

Daniel A. Obenchain: investigation (supporting), data curation (equal), formal analysis (equal), writing of original draft(equal)

Xuefang Xu: data curation (equal), formal analysis (equal), validation (equal), writing of original draft(equal)

Qian Gou: investigation (supporting), validation (equal), data curation (equal), formal analysis (equal), writing of original draft(equal), funding acquisition (lead), project administration (lead)

Walther Caminati: data curation (equal), formal analysis (equal), writing of original draft(equal)

Jens-Uwe Grabow: investigation (supporting), data curation (equal), formal analysis (equal), writing of original draft(equal)